AGU ADVANCING EARTH AND SPACE SCIENCE

Geophysical Research Letters

RESEARCH LETTER
10.1029/2020GL091074

Key Points:

- Strong lateral variations of lithosphere thickness is revealed roughly across the tectonic boundaries in eastern North America
- Multiple nearly parallel low-velocity layers are observed within the interior of the continental lithosphere of eastern North America
- The interior of the Grenville Province is characterized by strong variations of seismic characteristics from north to south

Supporting Information:

- Supporting Information S1

Correspondence to:
H. Gao,
haiyinggao@geo.umass.edu

Citation:
Gao, H., & Li, C. (2021). Lithospheric formation and evolution of eastern North American continent. *Geophysical Research Letters*, *48*, e2020GL091074. https://doi.org/10.1029/2020GL091074

Received 5 OCT 2020
Accepted 18 JAN 2021

Lithospheric Formation and Evolution of Eastern North American Continent

Haiying Gao[1] **and Cong Li**[1,2]

[1]Department of Geosciences, University of Massachusetts Amherst, Amherst, MA, USA, [2]Now at Department of Earth and Space Sciences, Southern University of Science and Technology, Shenzhen, Guangdong, China

Abstract Lithospheric layering contains critical information about continental formation and evolution. However, discrepancies on the depth distributions of lithospheric layers have significantly limited our understanding of possible tectonic connections among the layers. Here, we construct a high-resolution shear velocity model of eastern North America using full-wave ambient noise simulation and inversion by integrating onshore and offshore seismic datasets. Our new model reveals large lateral variations of lithosphere thickness approximately across the major tectonic boundaries, strong low-velocity anomalies underlying the thinner lithosphere, and multiple low-velocity layers within the continental lithosphere. We suggest that the present mantle lithosphere beneath eastern North America was formed and modified through multiple stages of tectonic processes, among which metasomatism may have significantly contributed to the observed intralithospheric low-velocity layers. The sharp thickness variation of lithosphere promoted edge-driven mantle convection, which has been consequently modifying the overlying mantle lithosphere and further sharpening the gradient of lithosphere thickness

Plain Language Summary Eastern North America provides a complete record of the eastward growth of the continent, from the breakup of one supercontinent (Rodinia), 1 billion years ago, through the multistage assembly of the supercontinent of Pangea to the formation of the modern Atlantic Ocean. Eastern North America provides an excellent setting to advance our understanding of lithosphere (i.e., tectonic plate) evolution through geologic time. Using an advanced seismic imaging method, we constructed a detailed model of the mantle lithosphere beneath eastern North America. Our new model demonstrates three key features: (1) strong lateral variations of lithosphere thickness from the North American craton (~200–250 km) to the Grenville Province (~150–200 km) and the Appalachian Province (~100 km); (2) multiple low-velocity layers within the continental lithosphere; and (3) low-velocity anomalies at the base of the Grenville and Appalachian lithosphere. Our seismic observations suggest that the eastern North American continent was likely established and modified through multiple stages of tectonic events. The sharp thickness variation of lithosphere triggered upwelling of deep mantle materials, which has been consequently modifying the overlying mantle lithosphere. Our findings shed light on the nature of mantle lithosphere and our understanding of continental growth and evolution in general.

1. Introduction

The physical properties (such as age, thickness, composition, temperature, and viscosity) of continental lithosphere contain crucial information about its formation and evolution, and more fundamentally, about Earth's tectonic dynamics through geological time. The thickness of cratonic lithosphere, revealed by fast seismic velocities, is on average ~200–250 km (e.g., Cammarano & Romanowicz, 2007; Bedle & van der Lee, 2009; Fischer et al., 2020; Hamza & Vieira, 2012; Kind et al., 2020; Schaeffer & Lebedev, 2014), roughly in agreement with estimates from xenolith analysis (O'Reilly & Griffin, 2010; Crépisson et al., 2014), heat flow (Mareschal & Jaupart, 2004), and magnetotelluric data (Adetunji et al., 2014; Evans et al., 2019). It is commonly agreed that cratonic lithosphere is thicker, colder, and more stable than younger continental lithosphere. The lithosphere-asthenosphere boundary (LAB) is typically interpreted as a thermal and rheologic transition zone (Sleep, 2005; Yuan & Romanowicz, 2010). Other factors, such as grain size, composition, water content, and extent of partial melt, may also contribute to the character of the LAB (Fischer et al., 2010).

Our understanding of the nature of continental lithosphere has been significantly evolved in recent years. A sharp seismic boundary has been detected within many cratons at a depth range of ~80–140 km (e.g., Eeken

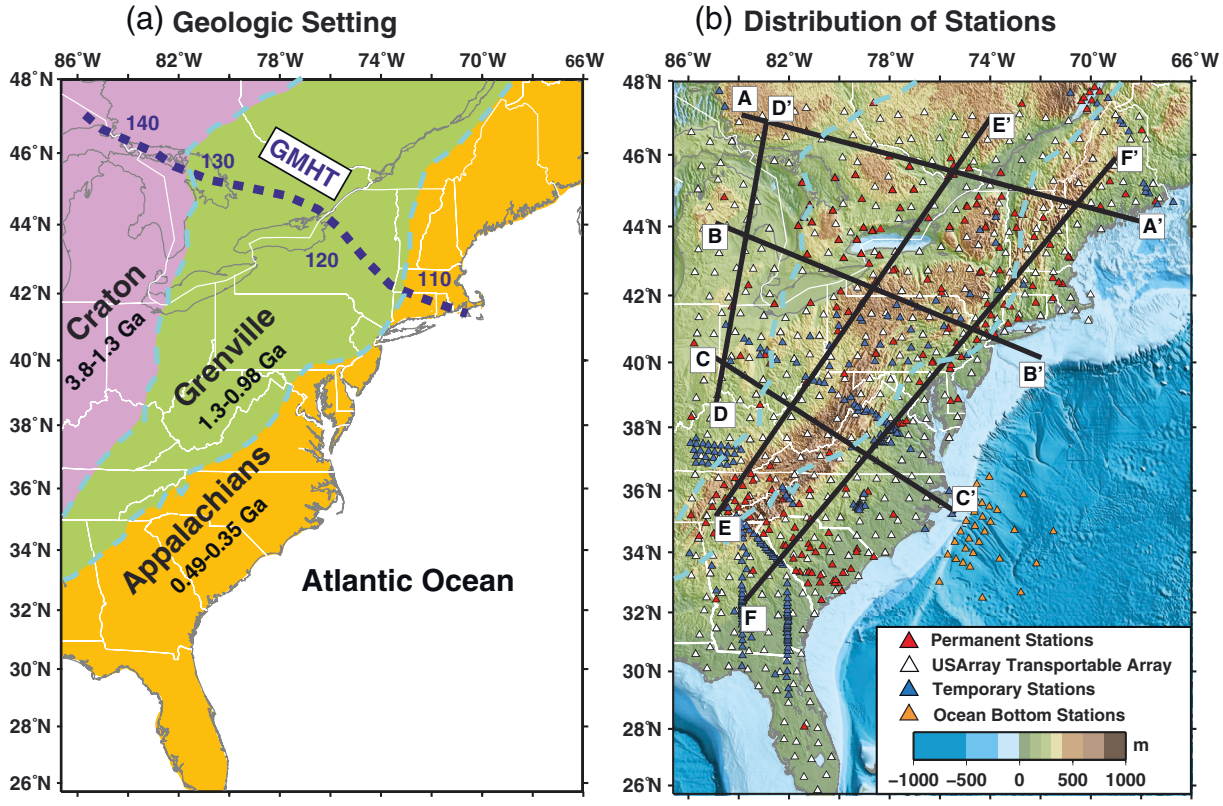

Figure 1. Major tectonic units in the eastern North American continent and distribution of seismic stations. (a) Three major tectonic units in eastern North America, modified after Hibbard et al. (2006). The two cyan dashed lines mark the inferred craton-Grenville boundary and the Grenville-Appalachian boundary. The blue dashed line indicates the Great Meteor hotspot track (GMHT), marked with time in Ma. (b) Distribution of seismic stations used in full-wave ambient noise tomography. The six black lines are the profile locations shown in Figures 2 and 3. GMHT, Great Meteor hotspot track.

et al., 2018; Hopper & Fischer, 2018; Petrescu et al., 2017; Rychert & Shearer, 2009; Yuan & Romanowicz, 2010). This type of boundary has been commonly termed as a mid-lithospheric discontinuity (MLD), and alternatively interpreted to reflect the presence of partial melting, seismic anisotropy, compositional variation, or a high geothermal gradient. However, the lithospheric boundaries, LAB and MLD, have typically been detected separately by independent seismological methods. The presence of MLD has not been imaged with tomographic methods, probably due to the lack of model resolutions on small-scale features. Discrepancies exist about the depth distribution and the sharpness of each layer, which significantly limit our understanding of the significance of the boundaries. For example, what are the possible tectonic connections among those boundaries? Was lithospheric layering inherited from the pre-existing architecture of continental lithosphere or newly developed after continental formation? How does the character of lithospheric layering change over geological time?

Eastern North America provides a complete record of continental evolution over the last 1.3 Ga from the formation and breakup of the supercontinent Rodinia through the multistage assembly of Pangea to the formation of the modern Atlantic Ocean (Hatcher, 2010; Thomas, 2006). This region involves three major tectonic units (Figure 1a), including the Archean North American craton (~3.8–1.3 Ga), the Proterozoic Grenville Province (~1.3–0.98 Ga), and the Paleozoic Appalachian orogen (~495–280 Ma) (David et al., 2009; Hatcher, 2010; McLelland et al., 2010, 2013), serving as an iconic setting to investigate the formation and modification of continental lithosphere. The coverage of seismic stations in eastern North America is excellent (Figure 1b), benefiting from the EarthScope Transportable Array (IRIS Transportable Array, 2003; UC San Diego, 2013), the Eastern North American Margin Community Seismic Experiment (Gaherty, 2014), together with many other seismic networks over the last 2 decades. The dense coverage of seismic stations provides us for the first time an unprecedented opportunity to construct a complete model of eastern North America. Using an advanced full-wave propagation simulation and inversion method, our new model

detects the coexistence of multiple intralithospheric low-velocity layers and sharp lateral variations of lithosphere thickness. The variations generally correlate with the major tectonic boundaries and thus, may relate to the accretionary tectonic history in eastern North America.

2. Data and Method

2.1. Extraction of Empirical Green's Functions

We collect ambient noise seismic waveforms from 1995 to 2019 recorded by 1,029 broadband stations in our study area (Figure 1b). We remove the instrument response, normalize the data with a frequency-time-normalization method (Shen et al., 2012), and eliminate waveform segments for large earthquakes. The Rayleigh-wave empirical Green's functions (EGF) are extracted from ambient noise cross-correlation of vertical-to-vertical components between each station pairs (Gao & Shen, 2014). We are able to retrieve high-quality Rayleigh-wave signals at periods up to 250 s (Figure S1), covering most of the eastern North American continent and part of the offshore region (Figure S2).

2.2. Finite-Difference Wave Simulation and Inversion

The full-wave propagation simulation and inversion have been fully documented by Gao and Shen (2014), Gao (2016, 2018), and Yang and Gao (2020). We simulate wave propagation in the three-dimensional (3-D) spherical Earth using the nonstaggered-grid, finite-difference method (Zhang et al., 2012). We parameterized the model domain into 0.035° × 0.035° in the longitudinal and latitudinal directions. The vertical grid size increases with depth from one-third of the horizontal grid size for the top 15 km to about 5 km at 100 km depth. The initial reference velocity model is the AK135 model extending from the surface down to 1,000 km depth. We extract the synthetic Rayleigh waveforms between each station pairs after wave simulation, and directly measure the phase delay times between the EGFs and synthetics by cross-correlation at multiple overlapping period bands, ranging from 150–250 s, 100–200 s, 75–150 s, 50–100 s, 35–75 s, 25–50 s, 15–35 s, 10–25 s, to 7–15 s. When measuring the phase delays, we require the signal-to-noise ratio of the EGFs to be ≥6 and the correlation coefficients to be ≥0.85.

We calculate the 3-D finite-frequency sensitivities of Rayleigh waves at the above period bands. The use of finite-frequency sensitivity kernels allows for the ability of resolving structures smaller than the dominant frequency (Spetzler & Snieder, 2004), which have been demonstrated by many previous studies (Chen et al., 2018; Gao & Shen, 2014; Tape et al., 2009; Wang et al., 2018, 2019). We consider the influence of both *P*- and *S*-wave velocities on the propagation of Rayleigh waves (Zhang et al., 2012; Zhang & Shen, 2008). Incorporation of *P*-wave velocities in kernel calculation and inversion provides additional constraints for the shallow crust, which significantly reduces the influence of *P*-wave velocity uncertainties on deeper structures. We invert for the shear velocity perturbations based on a damped least squares scheme (Montelli et al., 2004; Gao & Shen, 2014; Yang & Gao, 2020), with the damping and smoothing parameters selected in terms of the tradeoff between model norm and variance reduction (Figure S3). The velocity model was progressively and iteratively updated for a total of six iterations (Figures S4 and S5).

3. Results

Our new tomographic results (Figures 2 and 3) demonstrate three key features within one model system: (1) Strong lateral variations of lithosphere thickness from the North American craton (~200–250 km) to the Grenville Province (~150–200 km) and the Appalachian Province (~100 km); Here we define our interpreted LAB (thick transparent red lines in Figures 2 and 3) as the minimum negative gradient of velocity within a depth range of 150–260 km beneath the craton, 135–215 km beneath the Grenville, and 75–200 km beneath the Appalachians, respectively; (2) Multiple nearly horizontal low-velocity layers within the continental lithosphere; and (3) low-velocity anomalies at the base of the Grenville and Appalachian lithosphere. Please see supporting information for the average 1-D velocity profiles (Figure S6) and shear velocity maps at multiple depths (Figure S7). The checkerboard resolution tests (Figure S8) show that the model can be well recovered within a depth range of 50–250 km. The minimum resolvable dimensions increase from 55 km at shallower depths (≤75 km) to 135 km at greater depths (≥200 km). We also demonstrate that our

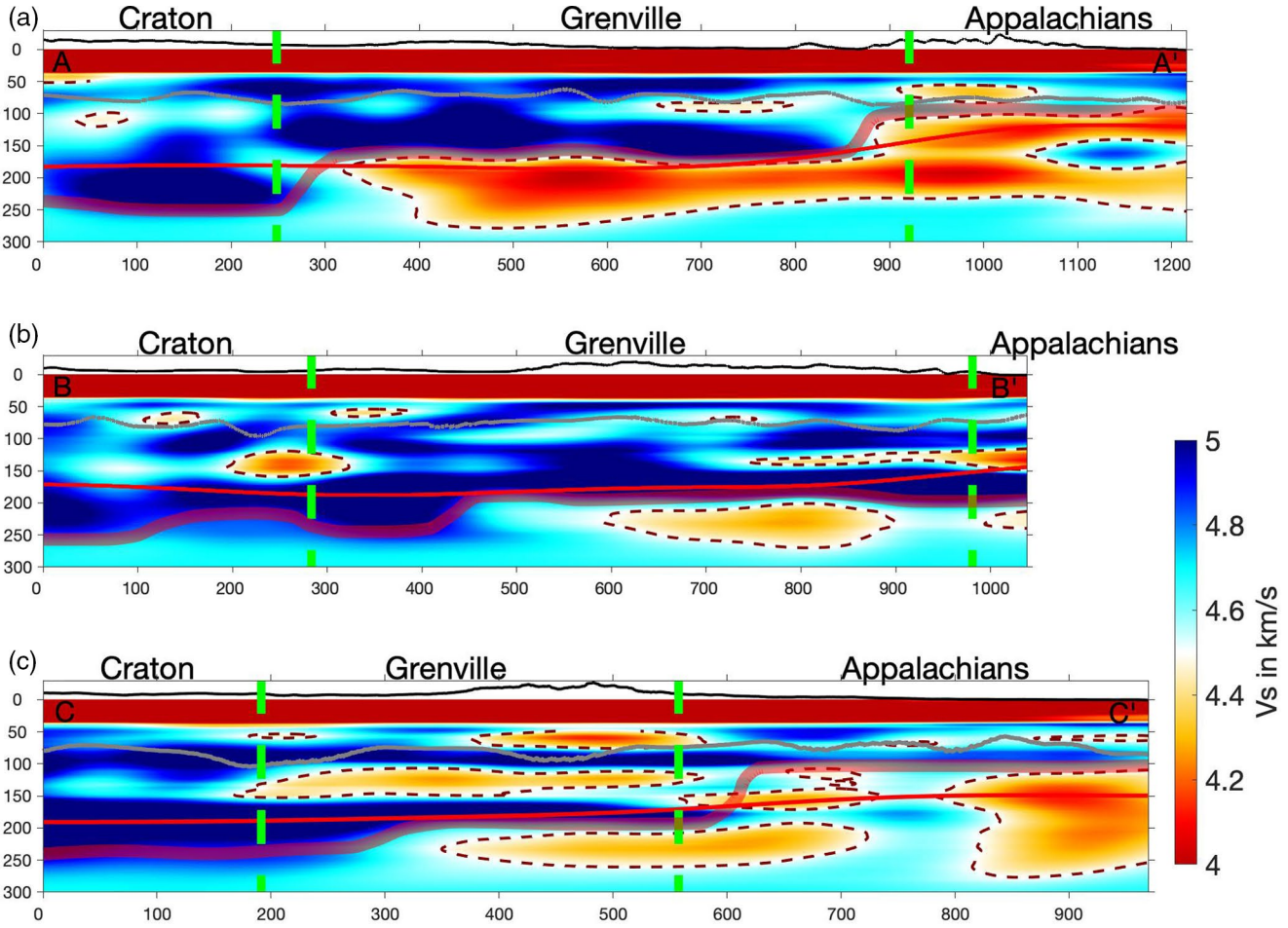

Figure 2. NW-SE profiles of the seismic tomography model beneath eastern North America. See profile locations in Figure 1b. The gray lines represent the sharp negative-wave speed discontinuity defined by teleseismic receiver functions (Hopper & Fischer, 2018). The thin red lines are the lithosphere-asthenosphere boundary defined by global tomography (Ho et al., 2016). The thick transparent red lines are our interpreted lithosphere-asthenosphere boundary. The brown dashed lines correspond to the Vs = 4.5 km/s contours. The two vertical dashed green lines mark the geologically defined surface boundaries between the three tectonic provinces. The black lines above each profile represent the bathymetry/topography.

model has the ability to resolve the lateral variation of lithosphere thickness among the major tectonic units (Figures S9–S13) and the intralithospheric low-velocity layers with the layer thickness greater than 25 km (Figures S14 and S15).

The new model is characterized by a fast velocity down to ~200–250 km depths beneath the craton (Figures 2 and 3a). We interpret this to reflect the thick continental lithosphere, consistent with previous seismic studies (e.g., Bedle & van der Lee, 2009; Biryol et al., 2016; Foster et al., 2020; Ho et al., 2016; Kind et al., 2020; Petrescu et al., 2017; Pollitz & Mooney, 2016; Schmandt & Lin, 2014; Yuan & Romanowicz, 2010). Within the cratonic lithosphere, we observe two thin low-velocity layers at a depth range of approximately 55–75 km and 125–155 km (Figure 3a), which appear to be nearly parallel to each other. The shear velocities of the two intracratonic layers vary within a range of ~4.5–4.6 km/s.

The interior of the Grenville Province is characterized by strong variations of seismic characteristics from north to south. First, a clear fast-to-slow velocity transition is observed at ~150–175 km depths beneath the northern Grenville and at ~200 km depth to the south, which we hypothesize as the base of the lithosphere. The thickness difference between the craton and the Grenville lithosphere results in a sharp offset up to 100 km in the north, which is located approximately along the geologically defined surface boundary (Figure 2a), and a relatively gradual 50-km offset in the south, which is about 100 km eastward of the surface boundary (Figure 2c). Second, we observe strong low-velocity anomalies (Vs < 4.4 km/s) located in the

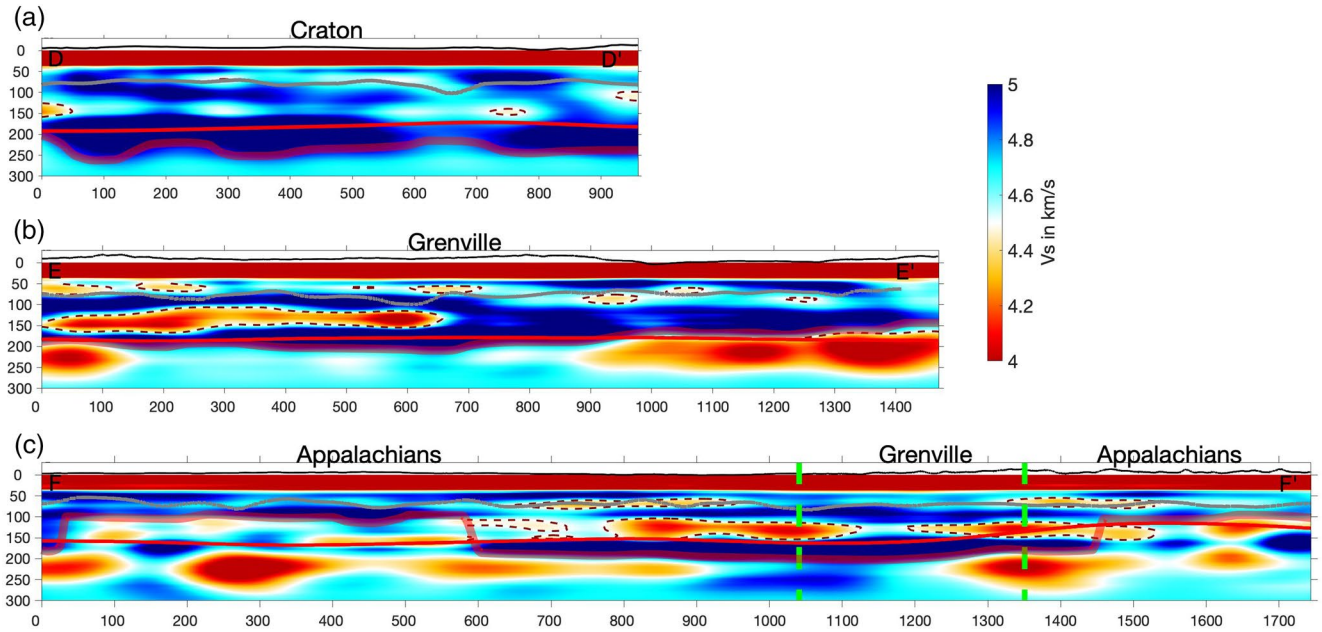

Figure 3. SW-NE profiles of the seismic tomography model beneath eastern North America. See profile locations in Figure 1b. Other symbols are the same as in Figure 2.

asthenosphere immediately beneath the southernmost and northern ends of the Grenville lithosphere (Figure 3b). In contrast, beneath the central segment of the Grenville lithosphere, the shear velocity is similar as the velocity beneath the craton. Third, we detect a nearly uniform low-velocity (~4.5–4.6 km/s) layer at a depth range of ~60–85 km within the northern Grenville lithosphere (Figure 3b). In contrast, two low-velocity layers are clearly imaged within the southern Grenville lithosphere. The top layer is located at a depth range of ~50–75 km with shear velocities of 4.4–4.5 km/s, and the bottom layer at depths of 125–155 km with much lower shear velocities (Vs < 4.4 km/s).

The seismic features in the Appalachian Province appear to be more complex and heterogeneous than within the craton and the Grenville Province. Beneath the northern and southern parts of the Appalachian Province, our model reveals a velocity reduction at the depth of ~100 km (Figures 2a and 2c), which we interpret as the base of the lithosphere (Hopper & Fischer, 2018; Wagner et al., 2018). Consequently, a sharp offset in lithospheric thickness (~75–100 km) is observed approximately at the Grenville - Appalachian surface boundary (Figures 2a and 2c). Strong low-velocity anomalies lie underneath the Appalachian lithosphere (Vs < 4.4 km/s; Figures 2a and 2c). In addition, a low-velocity (~4.5 km/s) layer is imaged at ~50–75 km depths. Finally, beneath the narrow segment of the central Appalachians, a strong low-velocity layer (Vs < 4.5 km/s) exists at ~125–150 km depths, underlain by a fast velocity down to ~200 km depth (Figures 2b and 3c).

The new tomographic model constrains, in significant detail, the distribution of both LAB and multiple intralithospheric layers beneath eastern North America. Even though numerous tomographic models exist for eastern North America (e.g., Bedle & van der Lee, 2009; Boyce et al., 2016; Boyce et al., 2019; Fichtner et al., 2018; Foster et al., 2020; Golos et al., 2018; Petrescu et al., 2017; Schaeffer & Lebedev, 2014; Yuan et al., 2014), none have the resolution and scope to detect the lithospheric features revealed in this study. Previous seismic anisotropy studies revealed an intracratonic boundary at the depths of ~120–150 km (e.g., Foster et al., 2020; Petrescu et al., 2017; Yuan & Romanowicz, 2010). Seismic receiver functions detect a boundary within a depth range of ~80–110 km (Hopper & Fischer, 2018; Liu & Stephen, 2018), which was interpreted as an MLD beneath the craton or as the LAB beneath the eastern North American margin. Our model clearly detects two nearly horizontal low-velocity layers within the craton and the U.S. Grenville lithosphere. The first layer roughly corresponds with the MLD that was previously detected by receiver functions (Hopper & Fischer, 2018; Liu & Stephen, 2018), and the second layer corresponds with the anisotropic

layer (Foster et al., 2020; Petrescu et al., 2017; Yuan & Romanowicz, 2010). In contrast, within the Canadian Grenville Province and the Appalachian Province, we image a single low-velocity layer, which roughly corresponds with the receiver-function-defined boundary (Hopper & Fischer, 2018; Liu & Stephen, 2018).

4. Discussion

Our model reveals strong structural variations within eastern North America. It has been demonstrated that more data and/or a more accurate methodology result in stronger velocity contrasts (e.g., Hung et al., 2004; Becker, 2012; Gao & Shen, 2014; Gao, 2018; Gao et al., 2020; Savage et al., 2017; Yang & Gao, 2020). Furthermore, we ignore seismic anisotropy and attenuation in wave simulation and inversion. Although this should not affect the key features discussed in this study, it may affect the amplitudes of shear velocity (e.g., Boyce et al., 2016; Debayle et al., 2020; Long et al., 2019). The shear velocity of the continental lithosphere within our study region varies within 4.6–4.8 km/s among different models of North America (Figure S6; e.g., Bedle & van der Lee, 2009; Yuan et al., 2014; Eeken et al., 2018), which is higher than the global models (e.g., Fichtner et al., 2018; Kennett et al., 1995). Here we define the reference velocity of continental lithosphere as the average of shear velocities within a depth range of 50–200 km (~4.7 km/s; Figure S6). The shear velocity of our model at the depths of ~200–250 km beneath the craton and ~100–150 km beneath the Grenville reaches up to 5.0 km/s, about 6% higher than the average of continental lithosphere. Similarly, Schaeffer and Lebedev (2014) demonstrated that the craton can be up to 8% higher than the average.

We suggest that the low-velocity layers observed within the continental lithosphere (Figures 2 and 3) likely represent the accumulation of fluid-rich minerals. In comparison with the average velocity of continental lithosphere (4.7 km/s), the intralithospheric low-velocity layers are about 2%–4% lower within the craton and the northern Grenville, and are at least 6% lower within the southern Grenville. Similarly, a velocity reduction up to 7%–10% across the MLD was also suggested by seismic receiver functions (Hopper & Fischer, 2018) and active-source seismic data (Ohira et al., 2017). Ohira et al. (2017) interpreted the MLD as a layer of partial melts frozen within the Pacific lithosphere. However, the preservation of partial melts within the old craton and Grenville Province is less likely. Alternatively, it has been commonly proposed that metasomatic alteration can significantly modify the mantle lithosphere of eastern North America (e.g., Boyce et al., 2016; Petrescu et al., 2017; Eeken et al., 2018; Boyce et al., 2019; Eeken et al., 2020; Foster et al., 2020). Metasomatized minerals formed at the depths of ~70–150 km can contain ~0.5–1 wt% of water, contributing to ~4–6% of shear velocity reduction (Eeken et al., 2018). The lateral discontinuity of the MLDs, which was also observed by receiver function studies (Hopper & Fischer, 2018; Liu & Stephen, 2018), suggests the irregular emplacement and accumulation of the hydrous minerals. Nevertheless, we cannot completely rule out contributions of other factors, such as seismic anisotropy and temperature (e.g., Eeken et al., 2020; Fischer et al., 2010).

A variety of mechanisms have been proposed for the seismically observed MLDs within North America. One hypothesis is that the craton was formed at (at least) two stages, with the top 100–150 km representing the Archean lithosphere and the lower part formed at a later stage (e.g., Altoe et al., 2020; Eeken et al., 2020; Foster et al., 2020; Petrescu et al., 2017; Yuan & Romanowicz, 2010). Another mechanism is that the entire craton was formed during the Archean, but its lower part was later modified by subduction-derived metasomatism (e.g., Boyce et al., 2016; Boyce et al., 2019). Alternatively, Perchuk et al. (2020) demonstrated that cratonic lithosphere can be thickened by large-scale viscous underplating of oceanic mantle during the Archean subduction. Below, we elaborate our preferred interpretations of the key seismic observations (Figure 4), although our model alone cannot differentiate those mechanisms or determine the timing(s) of formation/modification for each layer.

First, what are the origins of the intralithospheric low-velocity layers? It has been broadly suggested that the pre-existing structure at a lithospheric scale can be tectonically inherited through the cyclic assembly and breakup of supercontinent in eastern North America (Thomas, 2006; Wagner et al., 2018). We hypothesize that the mantle lithosphere (as well as the MLDs) was formed through multiple tectonic episodes. The lack of major large-scale tectonic events in eastern North America during the last 200 Ma helps to preserve the MLDs within the continental lithosphere. Specifically, the low-velocity layers located within a depth range of 50–85 km (Figure 4) were likely inherited from pre-existing lithosphere prior to the establishment of the

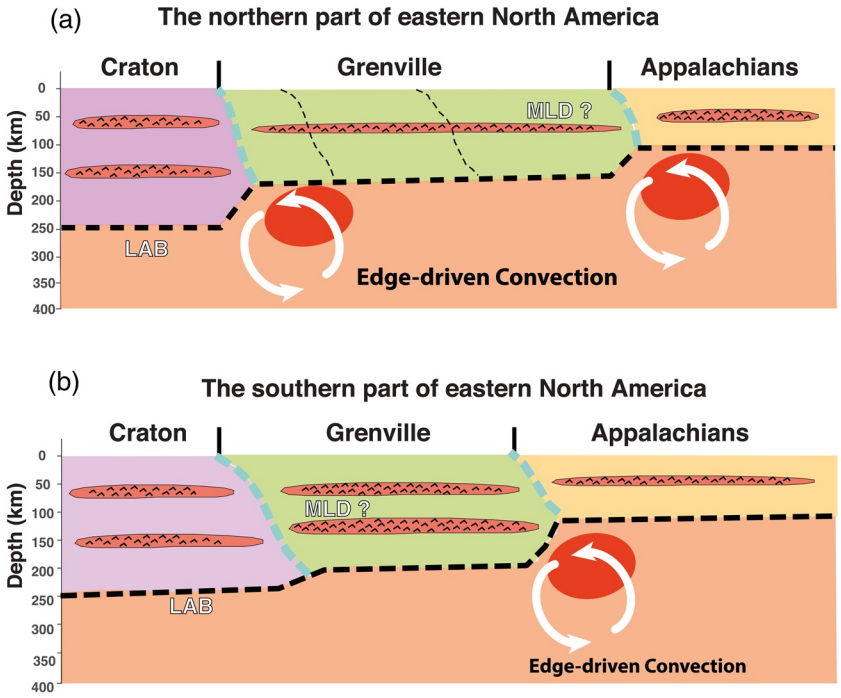

Figure 4. Schematic diagrams illustrating the key seismic features and possible interpretations in eastern North America. (a) Continent-arc collisional model that can be applied to the northern part of eastern North America. (b) Continent-continent collisional model that can be applied to the southern part of eastern North America. The thick black dashed lines represent the interpreted LAB. The cyan dashed lines represent our interpreted subsurface extent of the major tectonic boundaries. The nearly horizontal red patches with carets within the lithosphere denote the intralithospheric low-velocity layers. The red ellipses represent the observed low-velocity anomalies due to asthenosphere upwelling from edge-driven convection, and the white arrows denote the direction of edge-driven convection. The thin black dashed lines within the northern Grenville lithosphere mark the interpreted boundaries between small terranes. Modified after McLelland et al. (2010) and Li et al. (2020). LAB, lithosphere-asthenosphere boundary.

eastern North American continent. During the assembly of the supercontinents of Rodinia at ~1.3–0.98 Ga and Pangea at ~495-280 Ma, the lower part of the present mantle lithosphere was added beneath the Grenville and Appalachians, respectively. The subduction-derived metasomatism may contribute to the presence of the second low-velocity layers within the craton and southern Grenville lithosphere (Boyce et al., 2019). After the establishment of eastern North America, the mantle lithosphere would have experienced different levels of deformation and modification due to their inherent differences in strength/weakness (Audet & Bürgmann, 2010; Boyce et al., 2019; Wagner et al., 2018).

Second, what is the origin for the distinctive differences observed between the U.S. and Canadian portions of the Grenville Province? Those differences, ranging from crust to mantle lithosphere (Figure 3; e.g., Boyce et al., 2019; Eeken et al., 2020; Li et al., 2020; Schmandt et al., 2015; Shen & Ritzwoller, 2016), have important implications in terms of formation and/or modification of the Grenville lithosphere. The tomographic model by Boyce et al. (2019) showed that the cratonic lithosphere extends further eastward beneath the Canadian Grenville but is restricted to the west of the U.S. Grenville Front. In contrast, we observe a sharp difference in lithospheric thickness between the craton and the northern Grenville, which was also imaged by Boyce et al. (2016). We propose that the observed differences within the Grenville Province likely result from different modes of collision during the Grenville Orogeny. The Canadian Grenville represents the intense collision of a sequence of tectonic terranes onto the North American craton (Li et al., 2020; McLelland et al., 2013; Rivers, 1997). This intense collision may explain why the change of lithospheric thickness is approximately across the boundary between the craton and the Canadian Grenville (Figure 4). In addition, a portion of the northern Grenville Province passed over the Great Meteor hotspot at about 130–110 Ma (Figure 1a; Eaton & Frederiksen, 2007). The hotspot-induced mantle upwelling may have further thinned the

overlying lithosphere of the northern Grenville. In contrast, a simple continent-continent collision mode between the craton and the U.S. Grenville Province would likely result in the westward thrusting of Grenville lithosphere (Li et al., 2008, 2020; Long et al., 2019), supporting our observation in this study (Figure 4).

The sharp lateral variation of lithosphere thickness can initiate edge-driven mantle convection and asthenospheric upwelling (Figure 4; King & Anderson, 1998; Till et al., 2010), which would consequently modify the overlying mantle lithosphere and sharpen the gradient in lithosphere thickness. For example, the average seismic velocities beneath the Grenville and Appalachian lithosphere are much lower than beneath the craton (Figure S6), indicative of active mantle dynamics along the marginal lithosphere. The lateral extent of asthenospheric upwelling beneath the thinner lithosphere can reach up to 200 km (Till et al., 2010). Accumulation of melt produced by decompressional melting resulting from asthenospheric upwelling would significantly reduce the seismic velocities at the base of the thinner lithosphere (e.g., Chantel et al., 2016; Kawakatsu et al., 2009). The low-velocity anomalies at the base of the Grenville and Appalachian lithosphere can be up to 8%–10% lower than the average velocity (~4.6 km/s; Figure S6) beneath the craton, which would require the presence of at least 0.7% melt (Debayle et al., 2020). In addition, the hotspot-induced mantle upwelling may have further decreased the seismic velocities at the base of the northern Grenville lithosphere.

5. Conclusions

Continental accretion and evolution are fundamental questions of broad importance in Earth and Planetary sciences. The advanced full-wave propagation simulation and inversion provides a powerful tool to delineate the 3-D seismic features of the mantle lithosphere with great lateral and depth resolutions. Most importantly, our new model demonstrates strong lateral variations of lithosphere thickness and multiple nearly parallel low-velocity layers within the eastern North American lithosphere. We suggest that the present mantle lithosphere was likely formed and modified through multiple stages of tectonic processes. Among those tectonic processes, metasomatized minerals may have significantly contributed to the observed intralithospheric low-velocity layers. The sharp thickness variation of lithosphere initiated edge-driven mantle convection, which has been consequently modifying the overlying mantle lithosphere. Edge-driven mantle convection has also resulted in partial melts at the base of the Grenville and Appalachian lithosphere. These findings have implications for character of continental accretion in eastern Laurentia, the nature of mantle lithosphere, and our understanding of continental growth and evolution in general.

Data Availability Statement

All the continuous seismic data were requested via the Data Management Center (https://ds.iris.edu) of the Incorporated Research Institutions for Seismology (IRIS). The velocity model generated by this study is available through the IRIS Earth Model Collaboration (http://ds.iris.edu/ds/products/emc-ena_fwt2021/). The computer codes for full-wave ambient noise tomography were developed by Dr. Yang Shen at the University of Rhode Island (https://sites.google.com/view/seismo). The codes are available at Github open-access repository (https://doi.org/10.5281/zenodo.4021348).

Acknowledgments
This research was supported by the U.S. National Science Foundation under grant numbers EAR-1736167 and EAR-1930014. The computational resources used in this study were provided by the Massachusetts Green High Performance Computing Center. The authors thank Michael L. Williams for sharing his thoughts about possible implications of the tomographic models. The authors are grateful to two anonymous reviewers for their thoughtful comments that greatly improved the paper.

References

Adetunji, A. Q., Ferguson, I. J., & Jones, A. G. (2014). Crustal and lithospheric scale structures of the Precambrian Superior-Grenville margin. *Tectonophysics*, *614*, 146–169. https://doi.org/10.1016/j.tecto.2013.12.008

Altoe, I., Eeken, T., Goes, S., Foster, A., & Darbyshire, F. (2020). Thermo-compositional structure of the north-eastern Canadian Shield from Rayleigh wave dispersion analysis as a record of its tectonic history. *Earth and Planetary Science Letters*, *547*(1164650). https://doi.org/10.1016/j.epsl.2020.116465

Audet, P., & Bürgmann, R. (2010). Dominant role of tectonic inheritance in supercontinent cycles. *Nature Geoscience*, *4*. https://doi.org/10.1038/NGEO1080

Becker, T. W. (2012). On recent seismic tomography for the western United States. *Geochemistry, Geophysics, Geosystems*, *13*, Q01W10. https://doi.org/10.1029/2011GC003977

Bedle, H., & van der Lee, S. S. (2009). Velocity variations beneath North America. *Journal of Geophysical Research*, *114*, B07308. https://doi.org/10.1029/2008JB005949

Biryol, C. B., Wagner, L. S., Fischer, K. M., & Hawman, R. B. (2016). Relationship between observed upper mantle structures and recent tectonic activity across the Southeastern United States. *Journal of Geophysical Research: Solid Earth*, *121*, 3393–3414. https://doi.org/10.1002/2015JB012698

Boyce, A., Bastow, I. D., Darbyshire, F. A., Ellwood, A. G., Gilligan, A., Levin, V., et al. (2016). Subduction beneath Laurentia modified the eastern North American cratonic edge: Evidence from P wave and S wave tomography. *Journal of Geophysical Research: Solid Earth*, *121*, 5013–5030. https://doi.org/10.1002/2016JB012838

Boyce, A., Bastow, I. D., Golos, E. M., Rondenay, S., Burdick, S., & Van der Hilst, R. D. (2019). Variable modification of continental lithosphere during the Proterozoic Grenville orogeny: Evidence from teleseismic P-wave tomography. *Earth and Planetary Science Letters*, *525*. https://doi.org/10.1016/j.epsl.2019.115763

Cammarano, F., & Romanowicz, B. (2007). Insights into the nature of the transition zone from physically constrained inversion of long-period seismic data. *Proceedings of the National Academy of Sciences of the United States of America*, *104*, 9139–9144.

Chantel, J., Manthilake, G., Andrault, D., Novella, D., Yu, T., & Wang, Y. (2016). Experimental evidence supports mantle partial melting in the asthenosphere. *Science Advances*, *2*(5). e1600246. https://doi.org/10.1126/sciadv.1600246

Chen, M., Niu, F. L., Tromp, J., Lenardic, A., Lee, C. T. A., Cao, W. R., et al. (2018). Lithospheric foundering and underthrusting imaged beneath Tibet. *Nature Communications*, *9*. https://doi.org/10.1038/s41467-018-05925-8

Crépisson, C., Morard, G., Bureau, H., Prouteau, G., Morizet, Y., Petitgirara, S., et al. (2014). Magmas trapped at the continental lithosphere-asthenosphere boundary. *Earth and Planetary Science Letters*, *393*, 105–112. https://doi.org/10.1016/j.epsl.2014.02.048

David, J., Godin, L., Stevenson, R., O'Neil, J., & Francis, D. (2009). U-Pb ages (3.8-2.7 Ga) and Nd isotope data from the newly identified Eoarchean Nuvvuagittuq supracrustal belt, superior Craton, Canada. *The Geological Society of America Bulletin*, *121*(1–2), 150–163. https://doi.org/10.1130/B26369.1

Debayle, E., Bodin, T., Durand, S., & Ricard, Y. (2020). Seismic evidence for partial melt below tectonic plates. *Nature*, *586*(7830), 555–559. https://doi.org/10.1038/s41586-020-2809-4

Eaton, D. W., & Frederiksen, A. (2007). Seismic evidence for convection-driven motion of the North American plate. *Nature*, *446*(7134), 428–431. https://doi.org/10.1038/nature05675

Eeken, T., Goes, S., Pedersen, H. A., Arndt, N. T., & Bouilhol, P. (2018). Seismic evidence for depth-dependent metasomatism in cratons. *Earth and Planetary Science Letters*, *491*, 148–159. https://doi.org/10.1016/j.epsl.2018.03.018

Eeken, T., Goes, S., Petrescu, L., & Altoe, I. (2020). Lateral variations in thermochemical structure of the eastern Canadian shield. *Journal of Geophysical Research: Solid Earth*, *125*, e2019JB018734. https://doi.org/10.1029/2019JB018734

Evans, R. L., Benoit, M. H., Long, M. D., Elsenbeck, J., Ford, H. A., Zhu, J., et al. (2019). Thin lithosphere beneath the central Appalachian Mountains: A combined seismic and magnetotelluric study. *Earth and Planetary Science Letters*, *519*, 308–316. https://doi.org/10.1016/j.epsl.2019.04.046

Fichtner, A., van Herwaarden, D.-P., Afanasiev, M., Simute, S., Krischer, L., Cubuk-Sabuncu, Y., et al. (2018). The collaborative seismic earth model: Generation I. *Geophysical Research Letters*, *45*, 4007–4016. https://doi.org/10.1029/2018GL077338

Fischer, K. M., Ford, H. A., Abt, D. L., & Rychert, C. A. (2010). The lithosphere-asthenosphere boundary. *Annual Review of Earth and Planetary Sciences*, *38*(1), 551–575. https://doi.org/10.1146/annurev-earth-040809-152438

Fischer, K. M., Rychert, G. A., Dalton, C. A., Miller, M. S., Beghein, C., & Schutt, D. L. (2020). A comparison of oceanic and continental mantle lithosphere. *Physics of the Earth and Planetary Interiors*, *309*. https://doi.org/10.1016/j.pepi.2020.106600

Foster, A., Darbyshire, F., & Schaeffer, A. (2020). Anisotropic structure of the central North American Craton surrounding the Mid-Continent Rift: Evidence from Rayleigh waves. *Precambrian Research*, *342*(105662). https://doi.org/10.1016/j.precamres.2020.105662

Gaherty, J. B. (2014). *Eastern North American Margin community seismic experiment. International federation of digital seismograph networks*. https://doi.org/10.7914/SN/YO_2014

Gao, H. (2016). Seismic velocity structure of the Juan de Fuca and Gorda plates revealed by a joint inversion of ambient noise and regional earthquakes. *Geophysical Research Letters*, *43*, 5194–5201. https://doi.org/10.1002/2016GL069381

Gao, H. (2018). Three-dimensional variation of the slab geometry correlate with earthquake distributions at the Cascadia subduction system. *Nature Communications*, *9*, 1204. https://doi.org/10.1038/s41467-018-03655-5

Gao, H., & Shen, Y. (2014). Upper mantle structure of the Cascades from full-wave ambient noise tomography: Evidence for 3D mantle upwelling in the back-arc. *Earth and Planetary Science Letters*, *309*, 222–233. https://doi.org/10.1016/j.epsl.2014.01.012

Gao, H., Yang, X., Long, M. D., & Aragon, J. C. (2020). Seismic evidence for crustal modification beneath the Hartford rift basin in the northeastern United States. *Geophysical Research Letters*, *47*. e2020GL089316. https://doi.org/10.1029/2020GL089316

Golos, E. M., Fang, H., Yao, H., Zhang, H., Burdick, S., Vernon, F., et al. (2018). Shear wave tomography beneath the United States using a joint inversion of surface and body waves. *Journal of Geophysical Research: Solid Earth*, *123*(6), 5169–5189. https://doi.org/10.1029/2017JB014894

Hamza, V. M., & Vieira, F. P. (2012). Global distribution of the lithosphere-asthenosphere boundary: A new look. *Solid Earth*, *3*, 199–212. https://doi.org/10.5194/se-3-199-2012

Hatcher, R. D. (2010). The Appalachian orogen: A brief summary, from Rodinia to Pangea: The lithotectonic record of the Appalachian region. *Geological Society of America Memoir*, *206*, 1–19. https://doi.org/10.1130/2010.1206(01)

Hibbard, J. P., van Staal, C. R., Rankin, D. W., & Williams, H. (2006). *Lithotectonic map of the Appalachian orogen (MAP NO. 2096A, scale 1:5000000)*. Canada, United States of America: Geological Survey of Canada.

Ho, T., Priestley, K., & Debayle, E. (2016). A global horizontal shear velocity model of the upper mantle from multimode Love wave measurements. *Geophysical Journal International*, *207*(1), 542–561. https://doi.org/10.1093/gji/ggw292

Hopper, E., & Fischer, K. M. (2018). The changing face of the lithosphere-asthenosphere boundary: Imaging continental scale patterns in upper mantle structure across the contiguous U.S. with Sp converted waves. *Geochemistry, Geophysics, Geosystems*, *19*, 2593–2614. https://doi.org/10.1029/2018GC007476

Hung, S.-H., Shen, Y., & Chiao, L.-Y. (2004). Imaging seismic velocity structure beneath the Iceland hotspot - A finite-frequency approach. *Journal of Geophysical Research*, *109*, B08305. https://doi.org/10.1029/2003JB002889

IRIS Transportable Array. (2003). *USArray transportable Array: International federation of digital seismograph networks*. https://doi.org/10.7914/SN/TA

Kawakatsu, H., Kumar, P., Takei, Y., Shinohara, M., Kanazawa, T., Araki, E., et al. (2009). Seismic evidence for sharp lithosphere-asthenosphere boundaries of oceanic plates. *Science*, *324*(5926), 499–522. https://doi.org/10.1126/science.1169499

Kennett, B. L. N., Engdahl, E. R., & Buland, R. (1995). Constraints on seismic velocities in the earth from travel times. *Geophysical Journal International*, *122*, 108–124. https://doi.org/10.1111/j.1365-246X.1995.tb03540.x

Kind, R., Mooney, W. D., & Yuan, X. (2020). New insights into the structural elements of the upper mantle beneath the contiguous United States from S-to-P converted seismic waves. *Geophysical Journal International*, *222*, 646–659. https://doi.org/10.1093/gji/ggaa203

King, S. D., & Anderson, D. L. (1998). Edge-driven convection. *Earth and Planetary Science Letters*, *160*(3–4), 289–296. https://doi.org/10.1016/S0012-821X(98)00089-2

Li, C., Gao, H., & Williams, M. L. (2020). Seismic characteristics of the eastern North American crust with Ps converted waves: Terrane accretion and modification of continental crust. *Journal of Geophysical Research: Solid Earth*, *125*. https://doi.org/10.1029/2019JB018727
Li, Z. X., Bogdanova, S. V., Collins, A. S., Davidson, A., De Waele, B., Ernst, R. E., et al. (2008). Assembly, configuration, and break-up history of Rodinia: A synthesis. *Precambrian Research*, *160*(1–2), 179–210. https://doi.org/10.1016/j.precamres.2007.04.021
Liu, L., & Stephen, S. G. (2018). Lithospheric layering beneath the contiguous United States constrained by S-to-P receiver functions. *Earth and Planetary Science Letters*, *495*, 79–86. https://doi.org/10.1016/j.epsl.2018.05.012
Long, M. D., Benoit, M. H., Aragon, J. C., & King, S. D. (2019). Seismic imaging of mid-crustal structure beneath central and eastern North America: Possibly the elusive Grenville deformation? *Geology*, *47*(4), 371–374. https://doi.org/10.1130/G46077.1
Mareschal, J. C., & Jaupart, C. (2004). Variations of surface heat flow and lithospheric thermal structure beneath the North American craton. *Earth and Planetary Science Letters*, *223*, 65–77. https://doi.org/10.1016/j.epsl.2004.04.002
McLelland, J. M., Selleck, B. W., & Bickford, M. E. (2010). Review of the Proterozoic evolution of the Grenville Province, its Adirondack outlier, and the Mesoproterozoic inliers of the Appalachians. *Geological Society of America Memoir*, *206*(02), 21–49. https://doi.org/10.1130/2010.1206(02)
McLelland, J. M., Selleck, B. W., & Bickford, M. E. (2013). Tectonic evolution of the Adirondack Mountains and Grenville Orogen inliers within the USA. *Geoscience Canada*, *40*(4), 318. https://doi.org/10.12789/geocanj.2013.40.022
Montelli, R., Nolet, G., Masters, G., Dahlen, F. A., & Hung, S. H. (2004). Global P and PP traveltime tomography: Rays versus waves. *Geophysical Journal International*, *158*(2), 637–654. https://doi.org/10.1111/j.1365-246X.2004.02346.x
Ohira, A., Kodaira, S., Nakamura, Y., Fujie, G., Arai, R., & Miura, S. (2017). Evidence for frozen melts in the mid-lithosphere detected from active-source seismic data. *Scientific Reports*, *7*, 15770. https://doi.org/10.1038/s41598-017-16047-4
O'Reilly, S. Y., & Griffin, W. L. (2010). The continental lithosphere–asthenosphere boundary: Can we sample it? *Lithos*, *120*, 1–13. https://doi.org/10.1016/j.lithos.2010.03.016
Petrescu, L., Darbyshire, F., Bastow, I., Totten, E., & Gilligan, A. (2017). Seismic anisotropy of Precambrian lithosphere: Insights from Rayleigh wave tomography of the eastern superior craton. *Journal of Geophysical Research: Solid Earth*, *122*(5), 3754–3775. https://doi.org/10.1002/2016JB013599
Perchuk, A. L., Gerya, T. V., Zakharov, V. S., & Griffin, W. L. (2020). Building cratonic keels in Precambrian plate tectonics. *Nature*, *586*, 395–401. https://doi.org/10.1038/s41586-020-2806-7
Pollitz, F. F., & Mooney, W. D. (2016). Seismic velocity structure of the crust and shallow mantle of the Central and Eastern United States by seismic surface wave imaging. *Geophysical Research Letters*, *43*, 118–126. https://doi.org/10.1002/2015GL066637
Rivers, T. (1997). Lithotectonic elements of the Grenville Province: Review and tectonic implications. *Precambrian Research*, *86*(3–4), 117–154. https://doi.org/10.1016/S0301-9268(97)00038-7
Rychert, C. A., & Shearer, P. M. (2009). A global view of the lithosphere-asthenosphere boundary. *Science*, *324*, 495–498. https://doi.org/10.1126/science.1169754
San Diego, U. C. (2013). *Central and eastern US network*. International Federation of Digital Seismograph Networks. https://doi.org/10.7914/SN/N4
Savage, B., Covellone, B. M., & Shen, Y. (2017). Wave speed structure of the eastern North American margin. *Earth and Planetary Science Letters*, *459*, 394–405. https://doi.org/10.1016/j.epsl.2016.11.02
Schaeffer, A. J., & Lebedev, S. (2014). Imaging the North American continent using waveform inversion of global and USArray data. *Earth and Planetary Science Letters*, *402*, 26–41. http://dx.doi.org/10.1016/j.epsl.2014.05.014
Schmandt, B., & Lin, F.-C. (2014). P and S wave tomography of the mantle beneath the United States. *Geophysical Research Letters*, *41*, 6342–6349. https://doi.org/10.1002/2014GL061231
Schmandt, B., Lin, F. C., & Karlstrom, K. E. (2015). Distinct crustal isostasy trends east and west of the Rocky Mountain front. *Geophysical Research Letters*, *42*(10). 10290–10298. https://doi.org/10.1002/2015GL066593
Shen, W., & Ritzwoller, M. H. (2016). Crustal and uppermost mantle structure beneath the United States. *Journal of Geophysical Research: Solid Earth*, *121*, 4306–4342. https://doi.org/10.1002/2016JB012887
Shen, Y., Ren, Y., Gao, H., & Savage, B. (2012). An improved method to extract very-broadband empirical Green's functions from ambient seismic noise. *Bulletin of the Seismological Society of America*, *102*(4), 1872–1877. https://doi.org/10.1785/0120120023
Sleep, N. H. (2005). Evolution of the continental lithosphere. *Annual Review of Earth and Planetary Sciences*, *33*, 369–393. https://doi.org/10.1146/annurev.earth.33.092203.122643
Spetzler, J., & Snieder, R. (2004). The Fresnel volume and transmitted waves. *Geophysics*, *69*(3), 653–663. https://doi.org/10.1190/1.1759451
Tape, C., Liu, Q., Maggi, A., & Tromp, J. (2009). Adjoint tomography of the Southern California crust. *Science*, *325*(5943), 988–992. https://doi.org/10.1126/science.1175298
Thomas, W. A. (2006). Tectonic inheritance at a continental margin. *Geological Society of America Today*, *16*(2), 4–11. https://doi.org/10.1130/1052-5173(2006)016[4:TIAACM]2.0.CO;2
Till, C. B., Elkins-Tanton, L. T., & Fischer, K. M. (2010). A mechanism for low-extent melts at the lithosphere-asthenosphere boundary. *Geochemistry, Geophysics, Geosystems*, *11*, Q10015. https://doi.org/10.1029/2010GC003234
Wagner, L. S., Fischer, K. M., Hawman, R., Hopper, E., & Howell, D. (2018). The relative roles of inheritance and long-term passive margin lithospheric evolution on the modern structure and tectonic activity in the southeastern United States. *Geosphere*, *14*(4), 1385–1410. https://doi.org/10.1130/GES01593.1
Wang, K., Yang, Y. J., Basini, P., Tong, P., Tape, C., & Liu, Q. Y. (2018). Refined crustal and uppermost mantle structure of southern California by ambient noise adjoint tomography. *Geophysical Journal International*, *215*(2), 844–863. https://doi.org/10.1093/gji/ggy312
Wang, W., Chen, P., Keifer, I., Dueker, K., Lee, E. J., Mu, D. W., et al. (2019). Weathering front under a granite ridge revealed through full-3D seismic ambient-noise tomography. *Earth and Planetary Science Letters*, *509*, 66–77. https://doi.org/10.1016/j.epsl.2018.12.038
Yang, X., & Gao, H. (2020). Segmentation of the Aleutian-Alaska subduction zone revealed by full-wave ambient noise tomography: Implications for the along-strike variation of volcanism. *Journal of Geophysical Research: Solid Earth*, *125*(11). https://doi.org/10.1029/2020JB019677
Yuan, H., & Romanowicz, B. (2010). Lithospheric layering in the North American craton. *Nature*, *466*, 1063–1068. https://doi.org/10.1038/nature09332
Yuan, H., French, S., Cupillard, P., & Romanowicz, B. (2014). Lithospheric expression of geological units in central and eastern North America from full waveform tomography. *Earth and Planetary Science Letters*, *402*, 176–186. https://doi.org/10.1016/j.epsl.2013.11.057

Zhang, W., Shen, Y., & Zhao, L. (2012). Three-dimensional anisotropic seis- mic wave modeling in spherical coordinates by a collocated-grid finite-difference method. *Geophysical Journal International*, *188*, 1359–1381. https://doi.org/10.1111/j.1365-246X.2011.05331.x

Zhang, Z., & Shen, Y. (2008). Cross-dependence of finite-frequency compressional waveforms to shear seismic wave-speeds. *Geophysical Journal International*, *174*, 941–948. https://doi.org/10.1111/j.1365-246X.2008.03840.x